Supporting Information

Contents:

Experimental Methods and Preparation of Compounds

Experimental Conditions: Low temperature NMR Evans' Method of **1**

Table S1: Data used in calculating magnetic moment and molar susceptibility of **1** for low temperature NMR Evans' Method

Figure S1: Change in magnetic moment of **1** depending on temperature

Figure S2: ^{1}H NMR of **1** at different temperatures for Evans' Method analysis

Figure S3: ^{1}H NMR of $Cu_2[(2,4,6\text{-}Me_3C_6H_2N)_2C(H)]_2$

Figure S4: ^{13}C NMR of $Cu_2[(2,4,6\text{-}Me_3C_6H_2N)_2C(H)]_2$

Figure S5: ^{1}H NMR of **1**

Figure S6: ^{13}C NMR of **1**

Figure S7: Absorption Spectra for 0.3 mM $Cu_2[(2,4,6\text{-}Me_3C_6H_2N)_2C(H)]_2$ in dichloromethane

Figure S8: Absorption Spectra for **1** in dichloromethane at different concentrations

Figure S9: Cyclic Voltammogram of 0.1 M Bu_4NPF_6 in dichloromethane

Figure S10: Cyclic Voltammogram of 0.1 M Bu_4NPF_6 in THF

Figure S11: Cyclic Voltammogram of 1.48 mM $Cu_2[(2,4,6\text{-}Me_3C_6H_2N)_2C(H)]_2$ in dichloromethane

Figure S12: Cyclic Voltammogram of 0.63 mM $Cu_2[(2,4,6\text{-}Me_3C_6H_2N)_2C(H)]_2$ in THF

Figure S13: Infrared Spectrum of **1**

Figure S14: Infrared Spectrum of $Cu_2[(2,4,6\text{-}Me_3C_6H_2N)_2C(H)]_2$

Computational Methods and Optimized Coordinates

Figure S15: Solid-state structure of **1** determined by X-ray crystallography, with both disordered Cu_4S components shown.

Figure S16: ^{1}H-^{1}H COSY of **1**

Figure S17: ^{1}H NMR of **1** used for ^{1}H-^{1}H COSY experiment

Figure S18: EPR spectroscopy and temperature dependence

EXPERIMENTAL

General Considerations. Unless otherwise specified, all reactions and manipulations were performed under purified N_2 in a glovebox or using standard Schlenk line techniques. Glassware was oven-dried prior to use. Reaction solvents (diethyl ether, toluene, tetrahydrofuran, dichloromethane, acetonitrile, pentane) were sparged with argon and dried using a Glass Contour Solvent System built by Pure Process Technology, LLC. Chloroform was degassed, dried and distilled. Unless otherwise specified, all chemicals were purchased from commercial sources and used without further purification.

Physical Measurements. NMR spectra for compound characterization were recorded at ambient temperatures using Bruker Avance DPX-400 or Bruker Avance DRX-500 MHz spectrometers. Low temperature NMR spectra were recorded on a Bruker Avance DRX-500 MHz spectrometer and low temperatures were attained from liquid nitrogen boiloff. Equations (1) and (2) were used to calculate magnetic moment (B.M.) and molar susceptibility, respectively, using Evans' Method.

$$\mu_{eff} = \sqrt{8\ x\ X_m\ x\ T\ (K)} \qquad (1)$$

$$X_m = \frac{477\ x\ \Delta(Hz)}{2\ x\ Instrument\ frequency\ (Hz)\ x\ Molar\ concentration} \qquad (2)$$

^{1}H and ^{13}C NMR chemical shifts were referenced to residual solvent peaks. FT-IR spectra were recorded on solid samples in a glovebox using a Bruker ALPHA spectrometer fitted with a diamond-ATR detection unit. Elemental analyses were performed by the Midwest Microlab, LLC in Indianapolis, IN. Deuterated solvents were degassed by repeated freeze-pump-thaw

cycles and then stored over 3-Å molecular sieves. UV-Vis absorbance spectra were taken at room temperature using a Cary 300 Bio UV-Visible Spectrophotometer.

Electrochemical data was measured at room temperature using a WaveNow USB Potentiostat from Pine Research Instrumentation. In a classic three-electrode system, a platinum working electrode, platinum counter electrode and a $Ag/AgNO_3$ (0.01 M $AgNO_3$/0.1M Bu_4NPF_6 in THF or dichloromethane) reference electrode was used. Compound **1** was dissolved in a 0.1 M solution of Bu_4NPF_6 in THF or dichloromethane at approximately 1 mM concentrations. Electrochemical measurements were referenced to approximately 1mM solutions of $FeCp_2^{+/0}$ in same electrolyte solution.

X-band EPR spectra at 110 K to 150 K were obtained with a Bruker EMX spectrometer located at the National Biomedical EPR Center at the Medical College of Wisconsin. Spectra were simulated (not shown) with EasySpin[1] (Stoll, S.; Schweiger, A.J.; J. Magn. Reson., 2006, 78,42). Samples of 5 mM **1** were glassed in toluene spiked with 3-5 drops of dichloromethane. The full spectrum of **1** shown in the main text utilized microwave frequency 9.297 GHz, temp 115 K, 9 scans, microwave power 5 mW, mod. Amp. 5G, mod. Freq. 100 kHz, time constant 81.92 ms, sweep time 83.886 s. The insert focusing on the $g_{\|}$ region utilized microwave frequency 9.277 GHz, 25 scans, time constant 81.92 ms, sweep time 42.943 s.

X-ray crystallography. X-ray crystallography data was collected at the X-ray Structural Laboratory at Marquette University (Milwaukee, WI). The X-ray single-crystal diffraction data were collected with an Oxford Diffraction SuperNova diffractometer equipped with dual microfocus Cu/Mo X-ray sources, X-ray mirror optics, Atlas CCD detector and low-temperature

([1]) Stoll, S.; Schweiger, A.J. *J. Magn. Reson.* **2006**, *78*, 42

Cryojet device. Data was collected using Cu(Kα) radiation at 100 K. The data was processed with CrysAlisPro program package (Oxford Diffraction Ltd., 2010) typically using a numerical Gaussian absorption correction (based on the real shape of the crystal) followed by an empirical multi-scan correction using SCALE3 ABSPACK routine. The structures were solved using SHELXS program and refined with SHELXL program[2] within Olex2 crystallographic package.[3] All computations were performed on an Intel PC computer under Windows 7 OS. The structure contained a certain degree of disorder, as described in the main text, which was detected in difference Fourier syntheses of electron density and was taken care of using capabilities of SHELX package (see Figure S15 and caption for more information). Hydrogen atoms were localized in difference syntheses of electron density but were refined using appropriate geometric restrictions on the corresponding bond lengths and bond angles within a riding/rotating model (torsion angles of Me hydrogens were optimized to better fit the residual electron density). A solvent-mask procedure was applied to account for additional electron density that could not be assigned definitively to a co-crystallized solvent.

Preparation of Bis(2,4,6-trimethylphenyl)formamidine. A literature procedure was followed for the isolation of bis(2,4,6-trimethylphenyl)formamidine.[4] This synthesis took place in open air and acetone was used as the recrystallization solvent.

([2]) Sheldrick, G. M. *Acta Cryst*. **2008**, *A64*, 112–122.

([3]) Dolomanov, O. V.; Bourhis, L. J.; Gildea, R. J.; Howard, J. A. K.; Puschmann, H. *J. Appl. Cryst*. **2009**, *42*, 339–341.

([4]) Kolychev, E. L.; Portnyagin, I. A. ; Shuntikov, V. V.; Khrustalev, V. N.; Nechaev, M.S. *J. Organomet. Chem*. **2009,** *694,* 2454.

Preparation of $Cu_2[(2,4,6\text{-}Me_3C_6H_2N)_2C(H)]_2$. A modified version of the reported literature procedure for $Cu_2[(2,6\text{-}Me_2C_6H_3N)_2C(H)]_2$[5] was used as follows. Bis(2,4,6-trimethylphenyl)formamidine (1.83 g, 6.53 mmol) was dissolved in THF (approximately 120 mL). Sodium bis(trimethylsilyl)amide (1.34 g, 7.31mmol) was added to the stirring THF solution at room temperature, and the yellow solution was stirred for 1 h. Tetrakis(acetonitrile)copper(I) hexafluorophosphate (2.43 g, 6.52 mmol) was added to the stirring solution, which became instantly cloudy white. Stirring was continued at room temperature overnight. The solution volume was completely evaporated by vacuum. The evaporated residue was reconstituted in dichloromethane and filtered through Celite to remove insoluble $NaPF_6$. The resulting yellow filtrate was vacuum evaporated until a precipitate formed. This solid was collected by filtration and washed with diethyl ether (2 x 5 mL). The resulting white solid was dried under vacuum, and the filtrate was further vacuum evaporated to collect multiple crops. Yield of $Cu_2[(2,4,6\text{-}Me_3C_6H_2N)_2C(H)]_2$: 93%. ^{1}H NMR (400 MHz, $CDCl_3$): δ 2.21 (s, 12H, *p*-CH_3), 2.30 (s, 24H, *o*-CH_3), 6.79 (s, 8H, Ar C-H), 6.98 (s, 2H, NCH). $^{13}C\{^1H\}$ NMR (100 MHz, $CDCl_3$): δ 169.8 (NC(H)N), 144.4 (quat C, Ar), 133.4 (quat *p*-C, Ar), 132.8 (quat *o*-C, Ar), 128.7 (*m*-CH, Ar), 20.6 (Ar *p*-CH_3), 19.3 (Ar *o*-CH_3). FT-IR (cm^{-1}): 3002, 2903, 2848, 1611 (N=C), 1567, 1474, 1429, 1372, 1334, 1231, 1210, 1146, 1007, 846, 624, 583, 513, 418.

Preparation of $[Cu_4(\mu_4\text{-}S)(\mu_2\text{-}NCN)_4]$ (1) using S_8. $Cu_2[(2,4,6\text{-}Me_3C_6H_2N)_2C(H)]_2$ (0.300 g, 0.437 mmol) was dissolved in minimum amount of THF (~ 3 mL) using a magnetic stir bar. In a separate vessel, S_8 (0.007 g, 0.027 mmol) was stirred in 0.5 mL toluene until completely dissolved. The toluene solution of S_8 was then added to the $Cu_2[(2,4,6\text{-}Me_3C_6H_2N)_2C(H)]_2$

(5) Lane, A. C.; Vollmer, M. V.; Laber, C. H.; Melgarejo, D. Y.; Chiarella, G. M.; Fackler Jr., J. P.; Yang, X.; Baker, G. A.; Walensky, J. R. *Inorg. Chem.* **2014,** *53,* 11357.

solution dropwise, with stirring, at room temperature. Once all the S_8 solution had been added, the color began to change steadily to purple. The solution was stirred vigorously at 40-43° C overnight. The next day the solution was black. The solution was completely evaporated by vacuum. To the evaporated residue was added a small amount (~ 1 mL) of dichloromethane to make a super-saturated solution and was filtered. The dark solid was then washed with dichloromethane (2 x 4 mL) to remove unreacted $Cu_2[(2,4,6\text{-}Me_3C_6H_2N)_2C(H)]_2$, then diethyl ether (approximately 10 mL) to remove any remaining dichloromethane solvent, and finally acetonitrile (approximately 10 mL or until filtrate is clear) to remove a red-colored side product. Using a new, clean vacuum flask, the purple solid was extracted with copious amounts of dichloromethane until filtrate appeared clear. The purple filtrate was then pipette-filtered through Celite, and the solution was then completely evaporated under vacuum – after the filtrate is pipette-filtered through Celite, it should be evaporated as soon as possible to avoid decomposition into $Cu_2[(2,4,6\text{-}Me_3C_6H_2N)_2C(H)]_2$. Yield of **1**: 0.107 g, 34%. Compound **1** was stored in a freezer (-36°C) and is not stable in solution at room temperature for long periods of time. Note: Trace amounts (5-10%) of the starting material, ($Cu_2[(2,4,6\text{-}Me_3C_6H_2N)_2C(H)]_2$), were often detected by ^{1}H NMR regardless of multiple purification attempts. A good method for removing $Cu_2[(2,4,6\text{-}Me_3C_6H_2N)_2C(H)]_2$ is by adding a small amount of dichloromethane to the solid so that $Cu_2[(2,4,6\text{-}Me_3C_6H_2N)_2C(H)]_2$ dissolves but **1** is super-saturated and doesn't entirely dissolve. This solution is filtered, and the purple solid is washed with a small amount of dichloromethane and then diethyl ether to remove dichloromethane solvent. The purple solid can then be collected and dried under vacuum. Usually this purification method is done twice to achieve analytical purity. Dark black crystals may be obtained by dissolving purple **1** in a minimum amount of chloroform and allowing pentane vapors to diffuse in through a pin sized

hole. ^{1}H NMR (400 MHz, $CDCl_3$): δ 1.30 (s, 12 H, CH_3), 1.38 (s, 12 H, CH_3), 2.16 (s, 12 H, CH_3), 2.18 (s, 12 H, CH_3), 2.68 (s, 12 H, CH_3), 2.75 (s, 12 H, CH_3), 6.12 (s, 2 H, NC(H)N), 6.24 (s, 4 H, Ar CH), 6.30 (s, 4 H, Ar CH), 6.65 (s, 2 H, NC(H)N), 6.70 (s, 8 H, Ar CH). ^{13}C{^{1}H} NMR (100 MHz, $CDCl_3$): δ 172 (NC(H)N), 160 (NC(H)N), 144.5 (Ar), 144.3 (Ar), 133.6 (Ar), 133.4 (Ar), 132.7 (Ar), 132.58 (Ar), 132.53 (Ar), 128.7 (Ar), 128.5 (Ar), 128.2 (Ar), 128.0 (Ar), 21 (Ar *p*-CH_3), 20.7 (Ar *p*-CH_3), 20.4 (Ar *o*-CH_3), 18 (Ar *o*-CH_3), 17 (Ar *o*-CH_3). FT-IR (cm^{-1}): 2981, 2912, 2851, 1610 (N=C), 1553, 1530, 1471, 1372, 1339, 1325, 1224, 1206, 1144, 1029, 850, 735, 588, 571, 505, 460, 442, 412. Anal. calcd. for $C_{76}H_{92}Cu_4N_8S$: C, 65.0; H, 6.61; N, 7.98. Found: C, 64.91; H, 6.60; N, 8.06.

Preparation of [$Cu_4(\mu_4$-S)(μ_2-NCN)$_4$] (1) using Ph_3SbS. $Cu_2[(2,4,6\text{-}Me_3C_6H_2N)_2C(H)]_2$ (0.258 g, 0.376 mmol) was dissolved in minimum amount of THF (~ 3 mL) using a magnetic stir bar. In a separate vessel, Ph_3SbS (0.0727 g, 0.188 mmol) was dissolved in 2 mL THF. The solution of Ph_3SbS solution was then added to the $Cu_2[(2,4,6\text{-}Me_3C_6H_2N)_2C(H)]_2$ solution dropwise, with stirring, at room temperature. Once all the Ph_3SbS solution had been added, the color rapidly began to change from yellow to orange then maroon. The solution was stirred vigorously at room temperature overnight. The next day the solution was black. The solution was completely evaporated by vacuum. To the evaporated residue was added a small amount (~ 1 mL) of dichloromethane to make a super-saturated solution, which was filtered through Celite. The dark solid on the Celite pad was then washed with dichloromethane (2 x 6 mL) to remove unreacted $Cu_2[(2,4,6\text{-}Me_3C_6H_2N)_2C(H)]_2$, then diethyl ether (approximately 6 mL) to remove any remaining dichloromethane solvent, and finally acetonitrile (approximately 10 mL or until filtrate is clear) to remove any remaining triphenyl-antimony containing byproducts (usually appearing in ^{1}H NMR at δ 7.24- 7.15 ppm in $CDCl_3$). Using a new, clean vacuum flask, the

purple solid remaining on the Celite was collected with copious amounts of dichloromethane until the filtrate became clear (~ 100 mL). The dark purple filtrate was completely evaporated by vacuum. This filtrate should be evaporated as soon as possible to avoid decomposition into $Cu_2[(2,4,6\text{-}Me_3C_6H_2N)_2C(H)]_2$. Yield of **1**: 0.1144 g, 43%. Note: Trace amounts (5-10%) of the starting material, ($Cu_2[(2,4,6\text{-}Me_3C_6H_2N)_2C(H)]_2$), were often detected by ^1H NMR regardless of multiple purification attempts. The best method for removing $Cu_2[(2,4,6\text{-}Me_3C_6H_2N)_2C(H)]_2$ is by adding a small amount of dichloromethane to the solid so that $Cu_2[(2,4,6\text{-}Me_3C_6H_2N)_2C(H)]_2$ dissolves but **1** is super-saturated and doesn't entirely dissolve. This saturated solution is filtered, and the purple solid is washed with a small amount of dichloromethane and then diethyl ether to remove dichloromethane solvent. The purple solid can then be collected and dried under vacuum. Dark black crystals may be obtained by dissolving purple **1** in a minimum amount of chloroform and allowing pentane vapors to diffuse in through a pin sized hole.

Experimental Conditions: Low temperature NMR Evans' Method of **1**

$Cu_4S(NCN)_4$ (0.0015 g, 0.0010 mmol) was dissolved in $CDCl_3$ and 100 µL of $CHCl_3$ was added. Total weight of solution was 1.7571 g. The solution was then pipette-filtered through Celite into an NMR tube. A glass capillary tube (approximately 17 cm in length and approximately 3 mm in diameter) was syringe filled with $CHCl_3$ and then inserted into the NMR tube containing the $Cu_4S(NCN)_4$ solution. The difference in chloroform peak chemical shifts were analyzed to determine magnetic moment using Evans' Method.

Table S1: Data used in calculating magnetic moment and molar susceptibility of **1** for low temperature NMR Evans' Method.

Temperature (K)	Peak 1 (ppm)	Peak 2 (ppm)
298	7.272	7.259
280	7.274	7.261
261	7.275	7.262
240	7.275	7.262
221	7.274	7.262

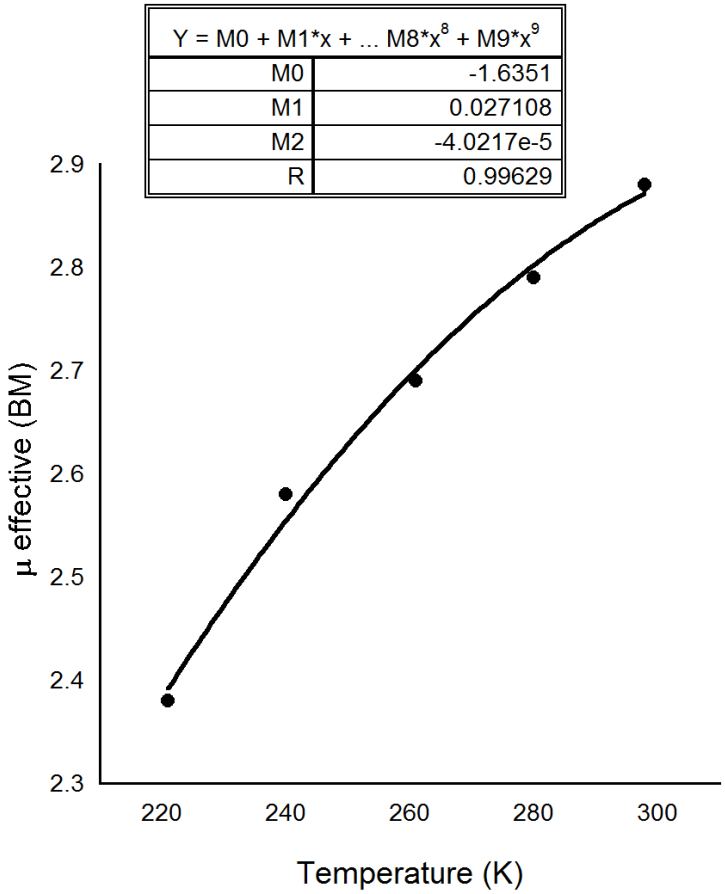

Figure S1: Change in magnetic moment of **1** depending on temperature studied by ^{1}H NMR Evans' Method analysis.

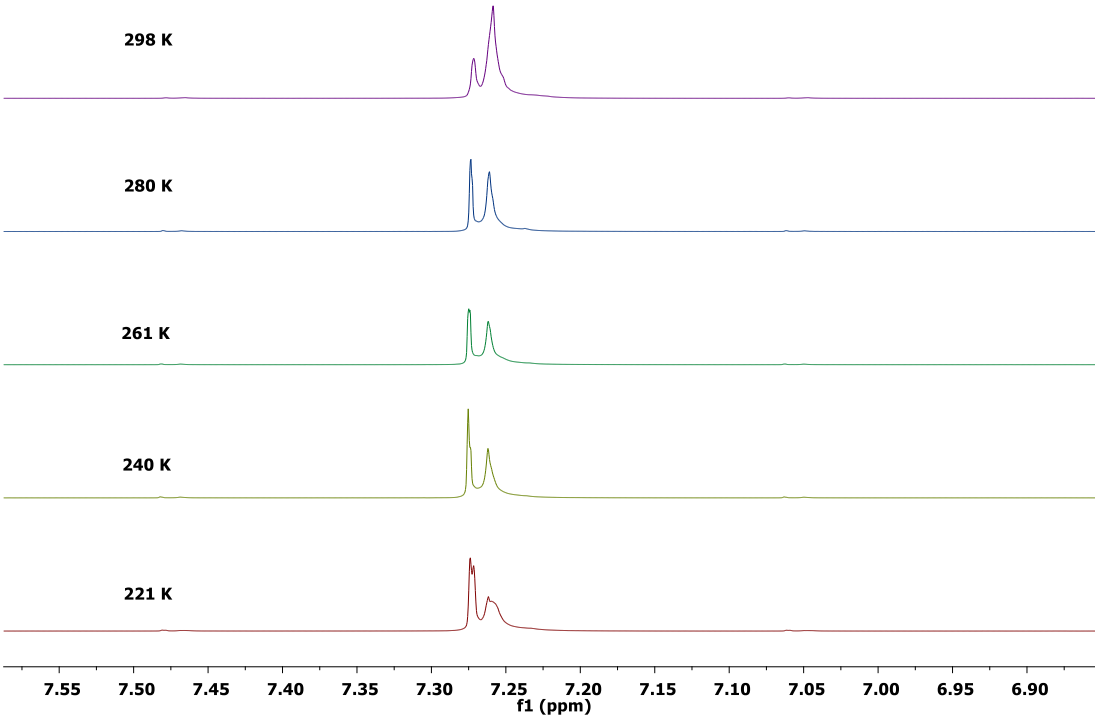

Figure S2: ^{1}H NMR (500 MHz) of **1** at different temperatures for Evans' Method analysis.

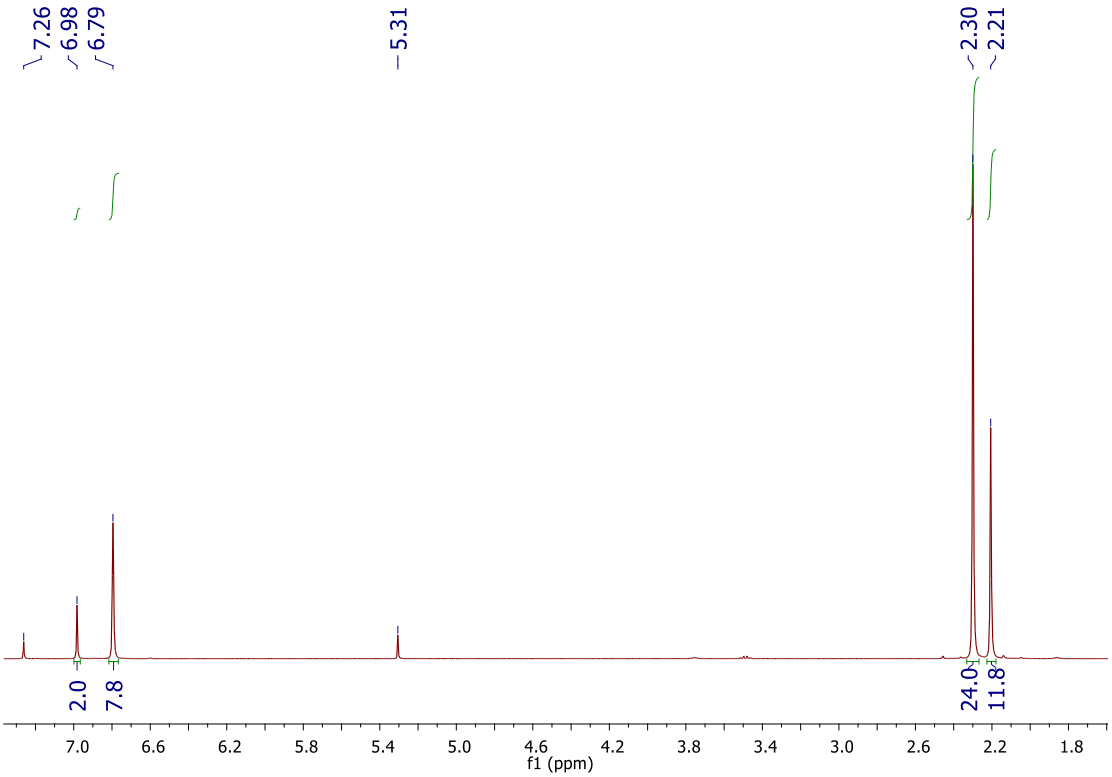

Figure S3. ^{1}H NMR (400 MHz) of $Cu_2[(2,4,6\text{-}Me_3C_6H_2N)_2C(H)]_2$ in $CDCl_3$. Peak observed at 5.31 ppm is residual dichloromethane.

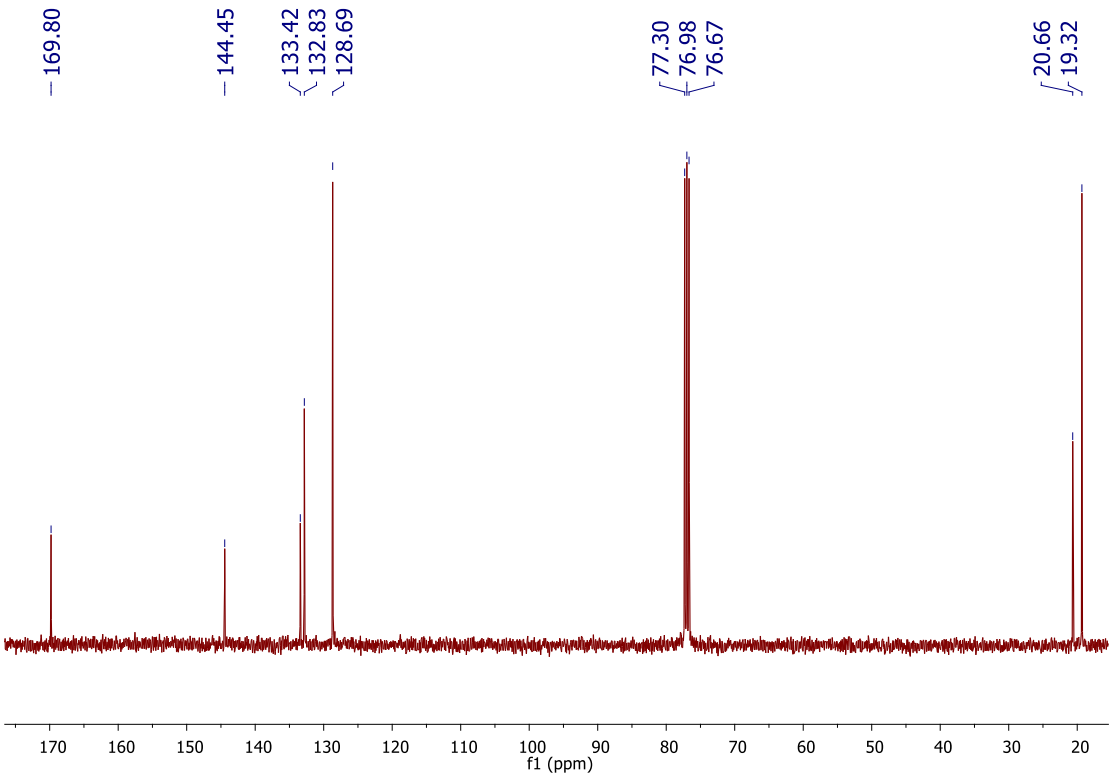

Figure S4. $^{13}C\{^{1}H\}$ NMR (100 MHz) of $Cu_2[(2,4,6\text{-}Me_3C_6H_2N)_2C(H)]_2$ in $CDCl_3$.

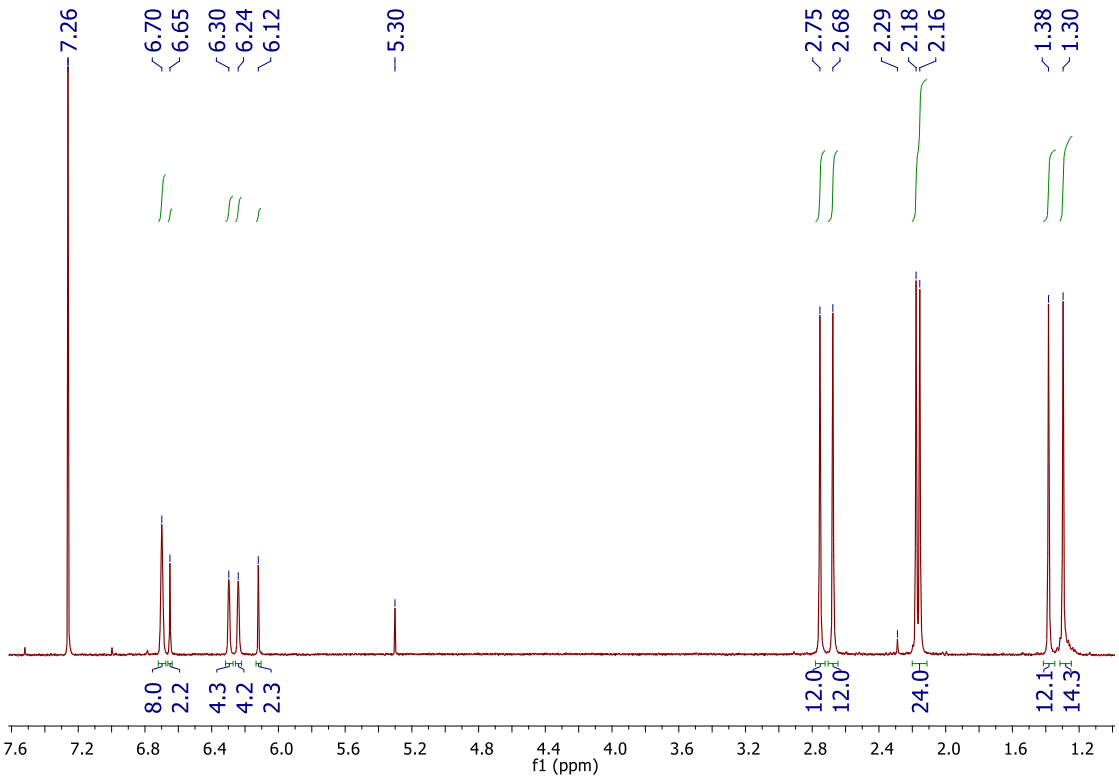

Figure S5: ^{1}H NMR (400 MHz) of **1** in $CDCl_3$. Peak observed at 5.30 ppm is residual dichloromethane. Peak observed at 2.29 ppm is trace amount of $Cu_2[(2,4,6\text{-}Me_3C_6H_2N)_2C(H)]_2$.

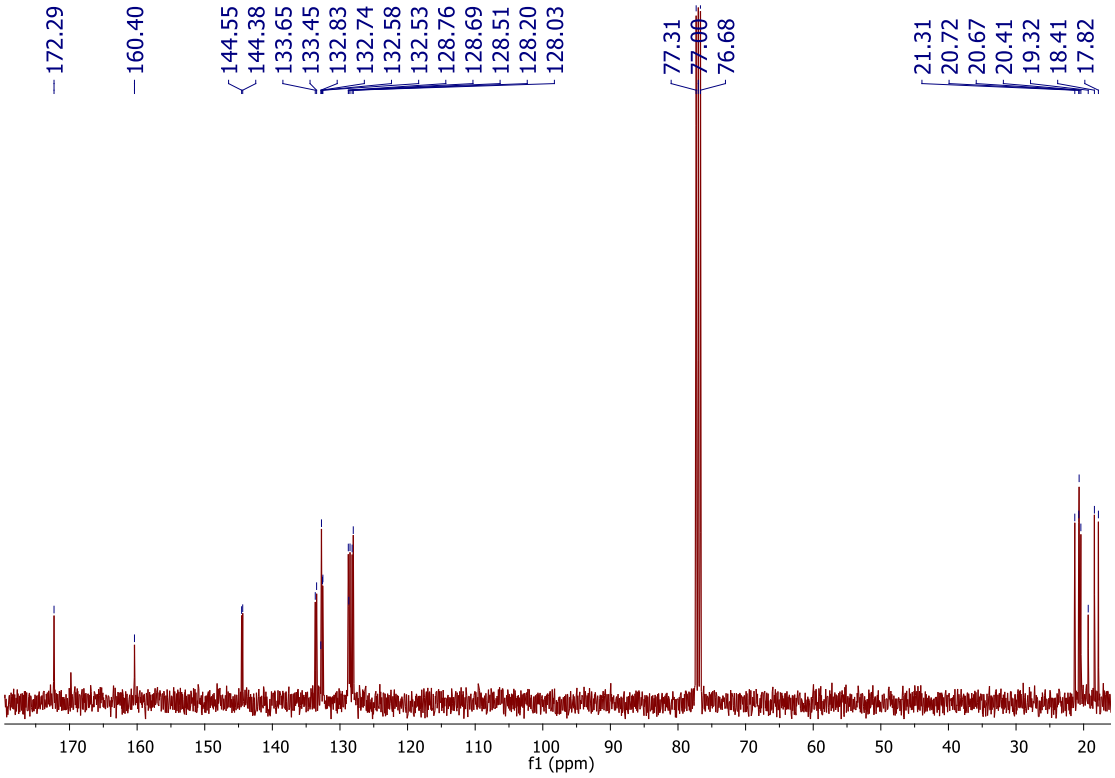

Figure S6: ^{13}C NMR (100 MHz) of **1** in $CDCl_3$. Peak observed at the following chemical shifts are residual amounts of $Cu_2[(2,4,6\text{-}Me_3C_6H_2N)_2C(H)]_2$; 132.8 ppm, 128.69 ppm, 20.67 ppm and 19.3 ppm.

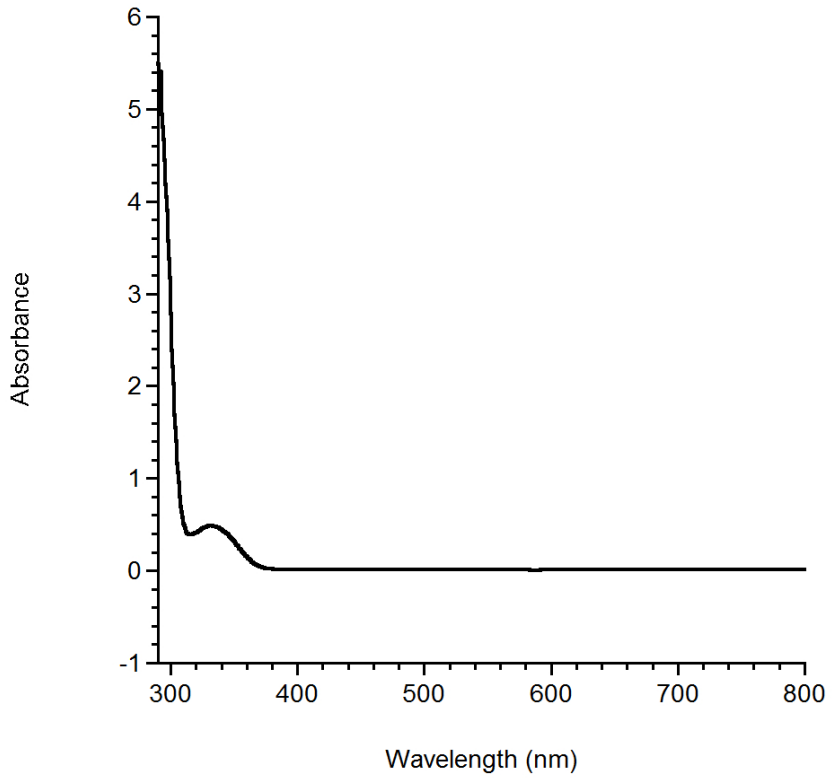

Figure S7: Absorption Spectra for 0.3 mM $Cu_2[(2,4,6\text{-}Me_3C_6H_2N)_2C(H)]_2$ in dichloromethane.

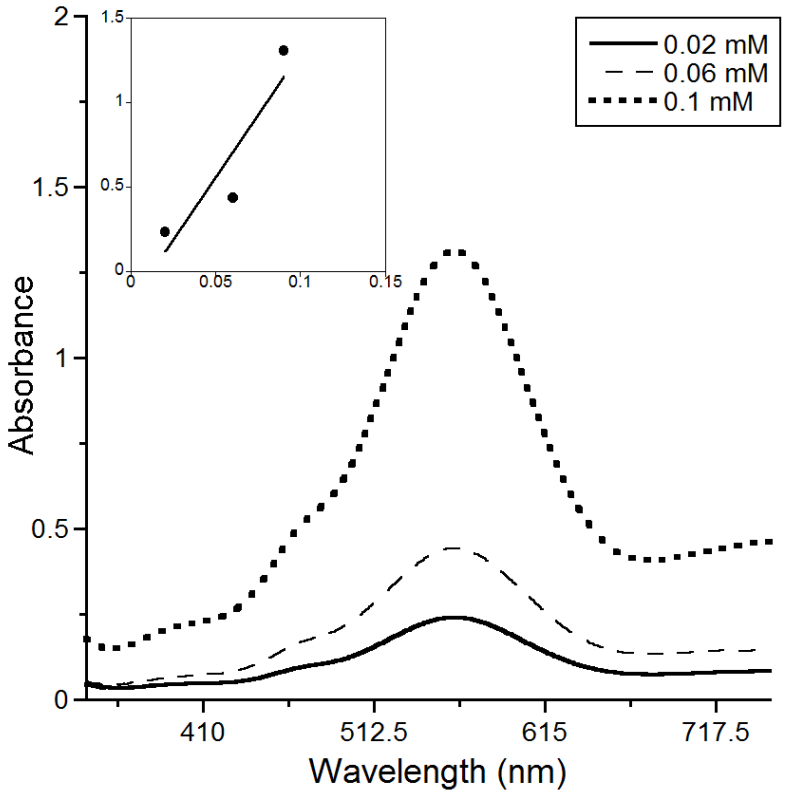

Figure S8: Absorption Spectra for **1** in dichloromethane at different concentrations. Inset plot of absorbance vs. concentration (mM); ε = 14000 M^{-1}•cm^{-1} (y = -0.1712 + 14.746x; R= 0.9100).

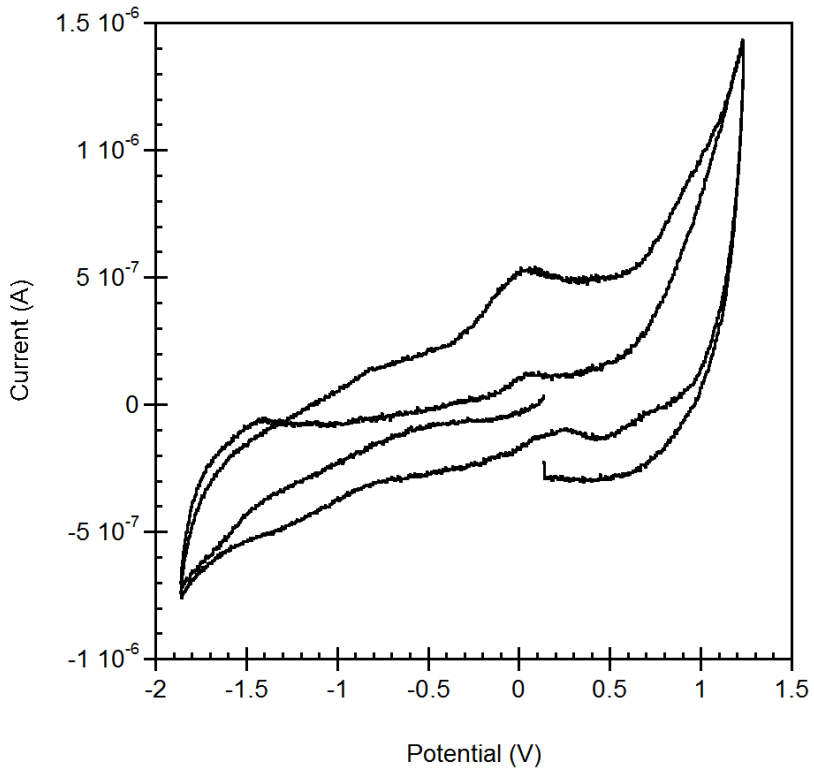

Figure S9: Cyclic Voltammogram of 0.1 M Bu_4NPF_6 background in dichloromethane vs $FeCp_2^{+/0}$.

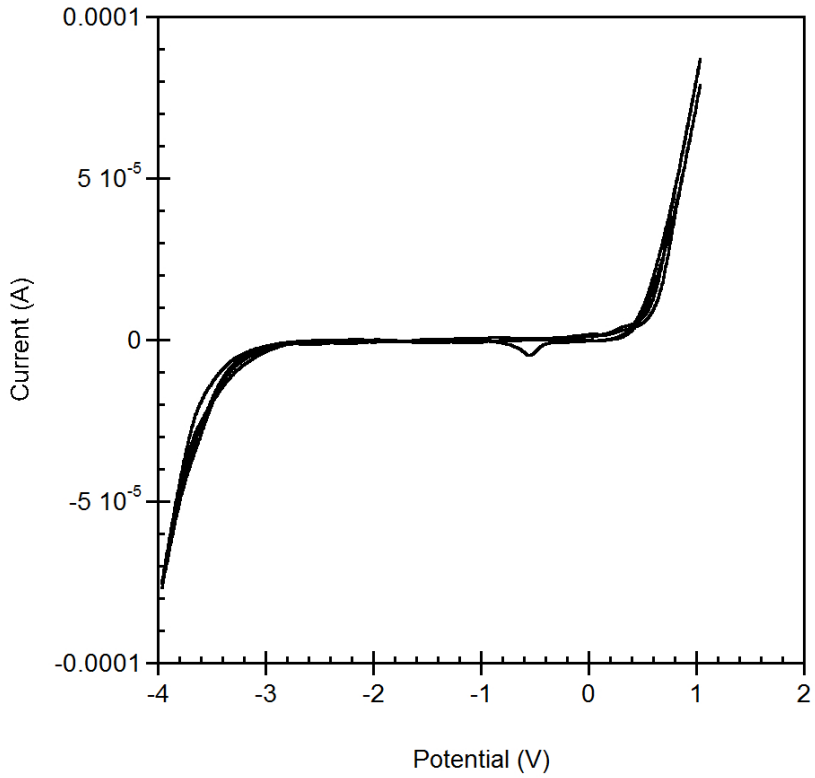

Figure S10: Cyclic Voltammogram of 0.1 M Bu_4NPF_6 background in THF vs. $FeCp_2^{+/0}$.

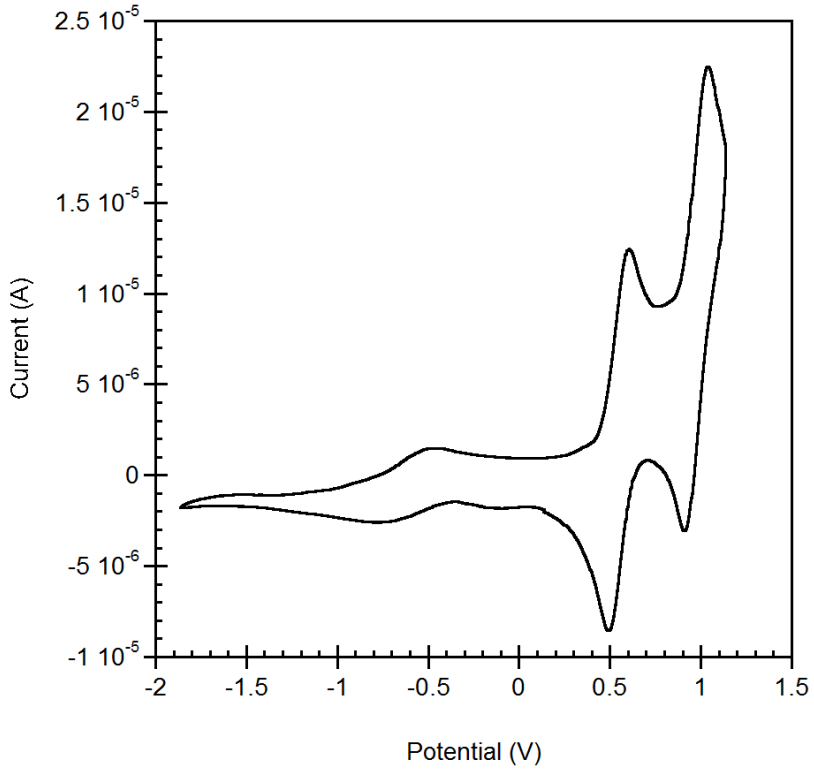

Figure S11: Cyclic Voltammogram of 1.48 mM $Cu_2[(2,4,6\text{-}Me_3C_6H_2N)_2C(H)]_2$ in dichloromethane vs. $FeCp_2^{+/0}$.

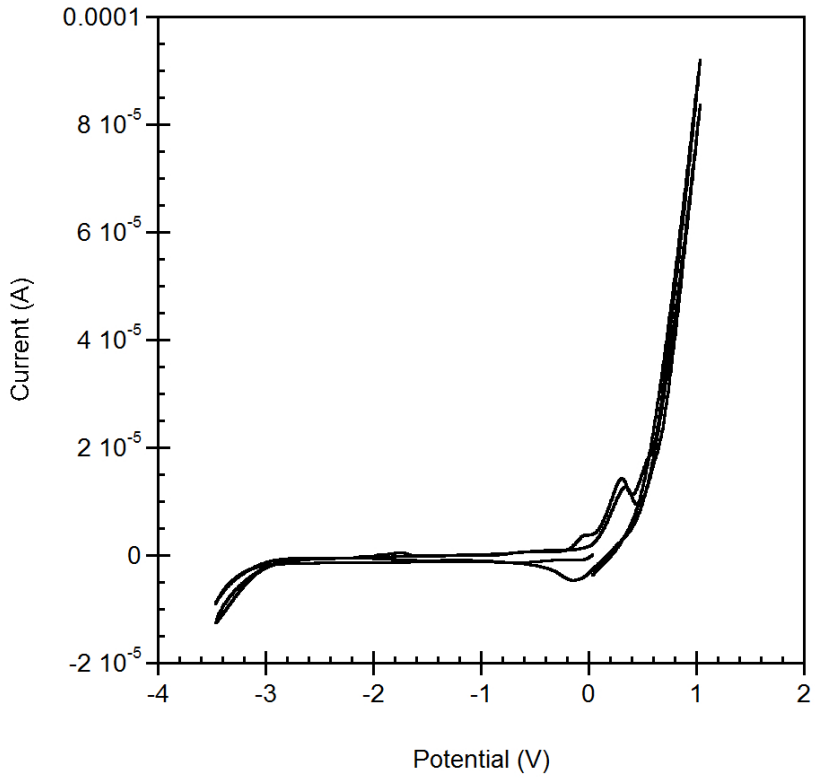

Figure S12: Cyclic Voltammogram of 0.63 mM $Cu_2[(2,4,6\text{-}Me_3C_6H_2N)_2C(H)]_2$ in THF vs. $FeCp_2^{+/0}$.

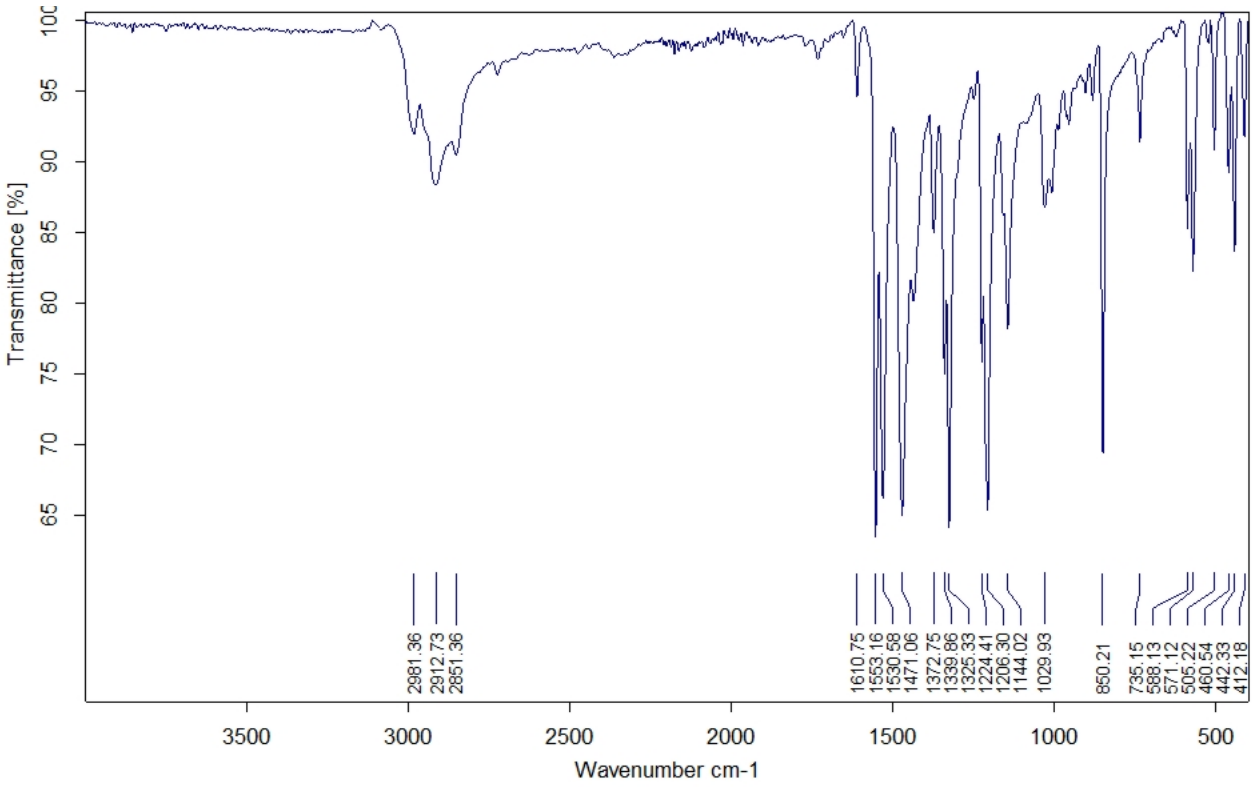

Figure S13: Infrared Spectrum of **1**.

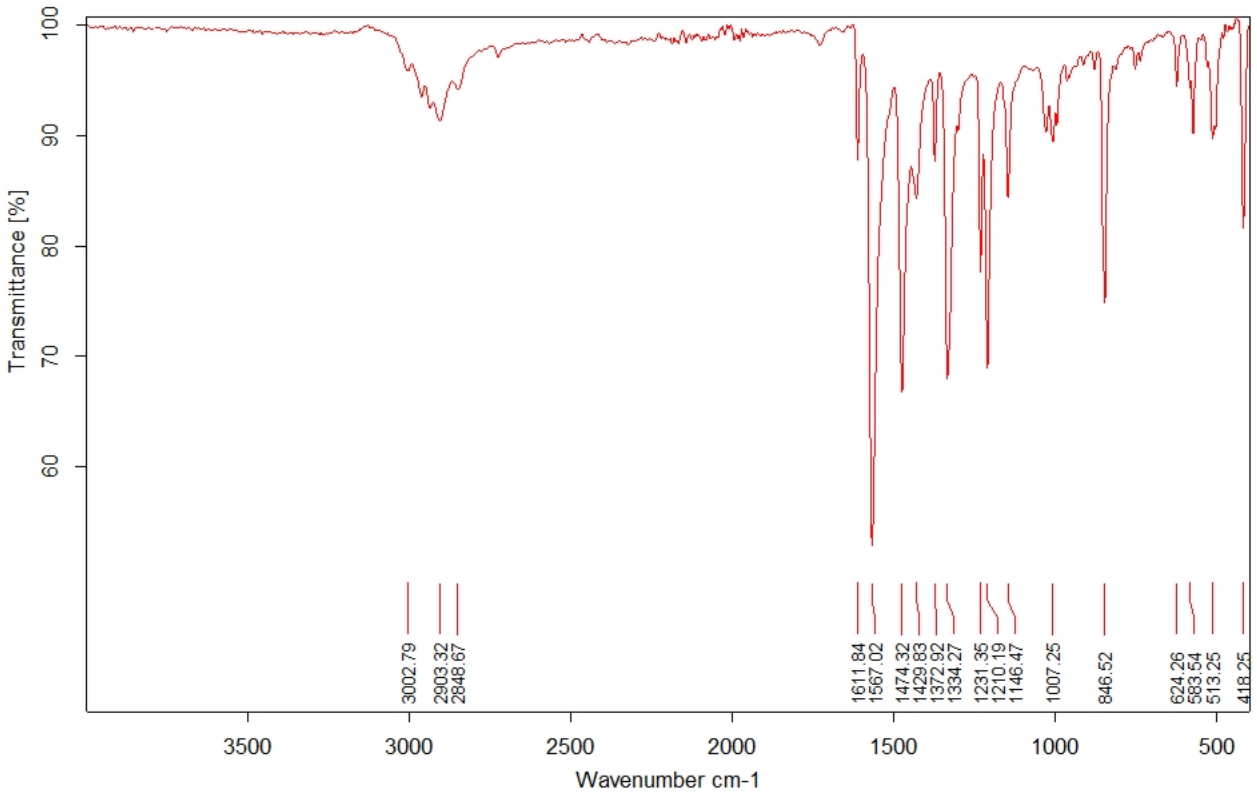

Figure S14: Infrared Spectrum of $Cu_2[(2,4,6\text{-}Me_3C_6H_2N)_2C(H)]_2$.

COMPUTATIONAL METHODS

All calculations were performed using Gaussian09, Revision B.01.[6] Density functional theory (DFT) calculations were carried out using a hybrid functional, BVP86, consisting of Becke's 1988 gradient-corrected Slater exchange functional[7] combined with the VWNS local electron correlation functional and Perdew's 1986 nonlocal electron correlation functional.[8] Mixed basis sets were employed: the LANL2TZ(f) triple-ζ basis set[9] with effective core potential[10] was used for Cu, the Gaussian09 internal 6-311+G(d) basis set was used for S, and the Gaussian09 internal 6-31+G(d) basis set was used for C, H, and N. The crystal structure of **1** was used as a starting point for constructing the input file: the mesityl groups were changed to methyl groups, and only one set of Cu_4S coordinates were used. All calculations were spin-unrestricted and symmetry-unrestricted. Final output wavefunctions were tested for stability against antiferromagnetic coupling (see: http://www.gaussian.com/g_tech/afc.htm) and were found to be stable. Orbital surfaces were analyzed using Gaussview, and orbital populations were determined using the Pop=Orbitals keyword in Gaussian09. Optimized coordinates for the singlet state of **1-Me** are enclosed below.

---

[6] Frisch, M. J.; Trucks, G. W.; Schlegel, H. B.; Scuseria, G. E.; Robb, M. A.; Cheeseman, J. R.; Scalmani, G.; Barone, V.; Mennucci, B.; Petersson, G. A.; Nakatsuji, H.; Caricato, M.; Li, X.; Hratchian, H. P.; Izmaylov, A. F.; Bloino, J.; Zheng, G.; Sonnenberg, J. L.; Hada, M.; Ehara, M.; Toyota, K.; Fukuda, R.; Hasegawa, J.; Ishida, M.; Nakajima, T.; Honda, Y.; Kitao, O.; Nakai, H.; Vreven, T.; Montgomery, J. A., Jr., Peralta, J. E.; Ogliaro, F.; Bearpark, M.; Heyd, J. J.; Brothers, E.; Kudin, K. N.; Staroverov, V. N.; Keith, T.; Kobayashi, R.; Normand, J.; Raghavachari, K.; Rendell, A.; Burant, J. C.; Iyengar, S. S.; Tomasi, J.; Cossi, M.; Rega, N.; Millam, J. M.; Klene, M.; Knox, J. E.; Cross, J. B.; Bakken, V.; Adamo, C.; Jaramillo, J.; Gomperts, R.; Stratmann, R. E.; Yazyev, O.; Austin, A. J.; Cammi, R.; Pomelli, C.; Ochterski, J. W.; Martin, R. L.; Morokuma, K.; Zakrzewski, V. G.; Voth, G. A.; Salvador, P.; Dannenberg, J. J.; Dapprich, S.; Daniels, A. D.; Farkas, O.; Foresman, J. B.; Ortiz, J. V.; Cioslowski, J.; , Fox, D. J. *Gaussian 09, Revision B.01; Gaussian*, Inc., Wallingford, CT, 2010.

[7] Becke, A. D. *Phys. Rev. A* **1988**, 38, 3098–100.

[8] Perdew, J. P. *Phys. Rev. B* **1986**, 33, 8822–24

[9] (a) Hay, P. J.; Wadt, W. R. *J. Chem. Phys.* **1985**, 82, 299. (b) Roy, L. E.; Hay, P. J.; Martin, R. L. *J. Chem. Theory Comput.* **2008**, 4, 1029. (c) Ehlers, A. W.; Bohme, M.; Dapprich, S.; Gobbi, A.; Hollwarth, A.; Jonas, V.; Kohler, K. F.; Stegmann, R.; Veldkamp, A.; Frenking, G. *Chem. Phys. Lett.* **1993**, 208, 111.

[10] (a) Hay, P. J.; Wadt, W. R. *J. Chem. Phys.* **1985**, 82, 270. (b) Hay, P. J.; Wadt, W. R. *J. Chem. Phys.* **1985**, 82, 284. (c) Hay, P. J.; Wadt, W. R. *J. Chem. Phys.* **1985**, 82, 299.

Cu1 Cu -1.3232 1.3228 -0.2204

S2 S 9.01401e-17 -0.0001 -1.472

Cu7 Cu 1.3231 -1.3227 -0.2202

Cu12 Cu 1.1189 1.4595 -0.15

N13 N 0.951 2.6674 1.375

N14 N -1.4014 2.5711 1.2715

C15 C -0.2624 2.9922 1.8152

H16 H -0.3289 3.6517 2.706

Cu17 Cu -1.1189 -1.4595 -0.1498

N18 N -0.9509 -2.6671 1.3754

N19 N 1.4016 -2.5707 1.2719

C20 C 0.2626 -2.992 1.8156

H21 H 0.3291 -3.6515 2.7063

C30 C 2.1006 3.2074 2.094

H31 H 2.8286 2.4073 2.3177

H32 H 2.6238 3.98 1.4974

H33 H 1.7988 3.6724 3.0545

C34 C -2.654 3.0268 1.8641

H35 H -3.345 2.1765 2.0013

H36 H -2.4893 3.5005 2.8533

H37 H -3.1614 3.7695 1.2166

C46 C -2.1005 -3.2072 2.0944

H47 H -1.7986 -3.6726 3.0547

H48 H -2.8283 -2.407 2.3185

H49 H -2.624 -3.9794 1.4976

C50 C 2.6542 -3.0266 1.8644

H51 H 2.4896 -3.5002 2.8536

H52 H 3.1615 -3.7693 1.2168

H53 H 3.3453 -2.1763 2.0014

N3 N -3.1307 0.9736 -0.9666

N4 N -2.9782 -1.3951 -0.8587

C5 C -3.5863 -0.257 -1.1737

H6 H -4.5845 -0.3419 -1.6504

C38 C -3.9049 2.0935 -1.4931

H39 H -4.8927 1.7673 -1.8774

H40 H -4.082 2.8517 -0.7085

H41 H -3.3694 2.5931 -2.3242

C42 C -3.6538 -2.647 -1.1882

H43 H -3.8477 -3.2471 -0.2795

H44 H -4.6269 -2.4703 -1.6895

H45 H -3.0327 -3.2617 -1.867

N8 N 3.1306 -0.9739 -0.9666

N9 N 2.9783 1.3948 -0.8589

C10 C 3.5862 0.2567 -1.1738

H11 H 4.5844 0.3415 -1.6506

C22 C 3.9042 -2.0938 -1.494

H23 H 4.0794 -2.8534 -0.7103

H24 H 3.3694 -2.5915 -2.3266

H25 H 4.893 -1.7681 -1.8762

C26 C 3.6542 2.6467 -1.1877

H27 H 4.6266 2.4699 -1.6904

H28 H 3.0326 3.2625 -1.865

H29 H 3.8496 3.2457 -0.2786

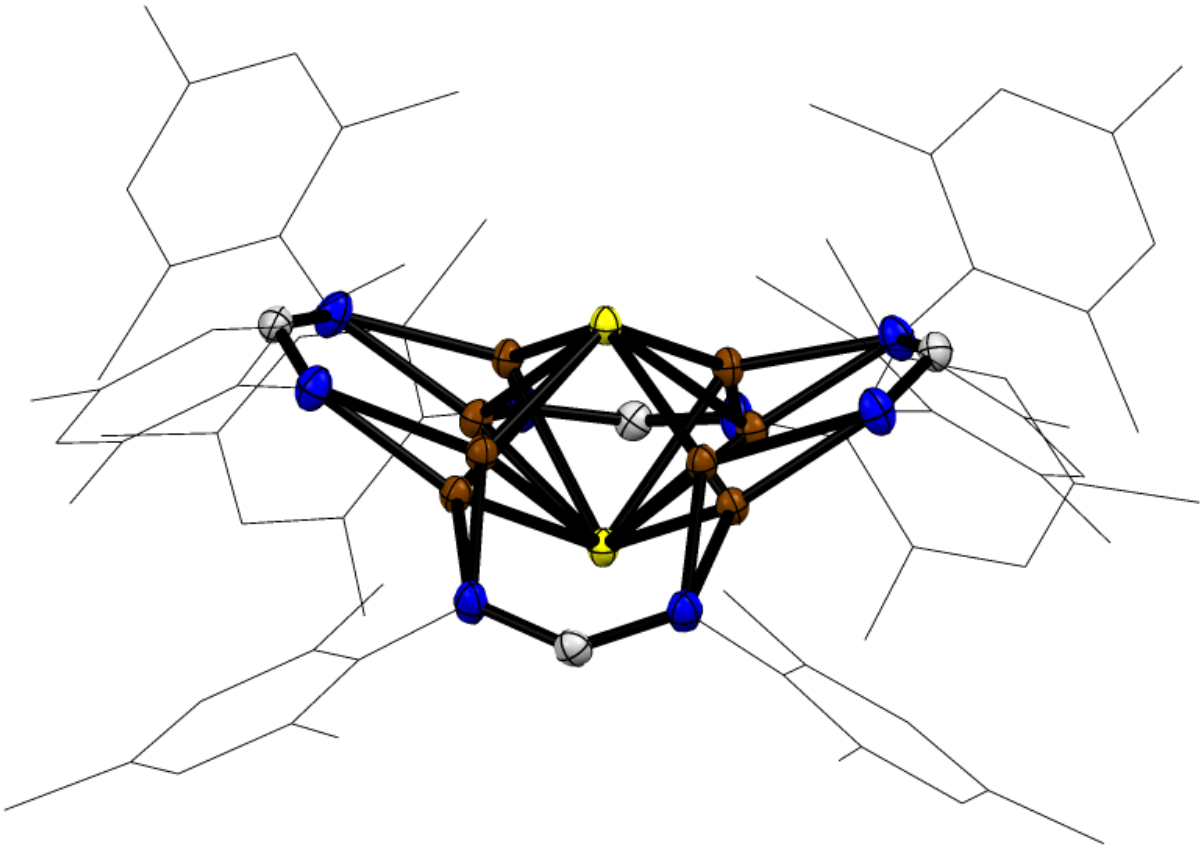

Figure S15. Solid-state structure of **1** determined by X-ray crystallography, with both disordered Cu_4S components shown. The molecule is positioned on crystallographic element of symmetry (-4) and experiences two types of disorder: (a) the S cap alternatively occupies 2 symmetrically equivalent position over and under the Cu_4 moiety, and (b) each of the Cu ions of the central moiety deviates alternatively up or down from the mean plane that corresponds to a superposition of two tetrahedral distortions of opposite sign. The ligands do not show any perceptible disorder. Apparently, they form a significantly robust scaffold around the central metal nucleus owing to stacking between their overlapping mesityl groups.

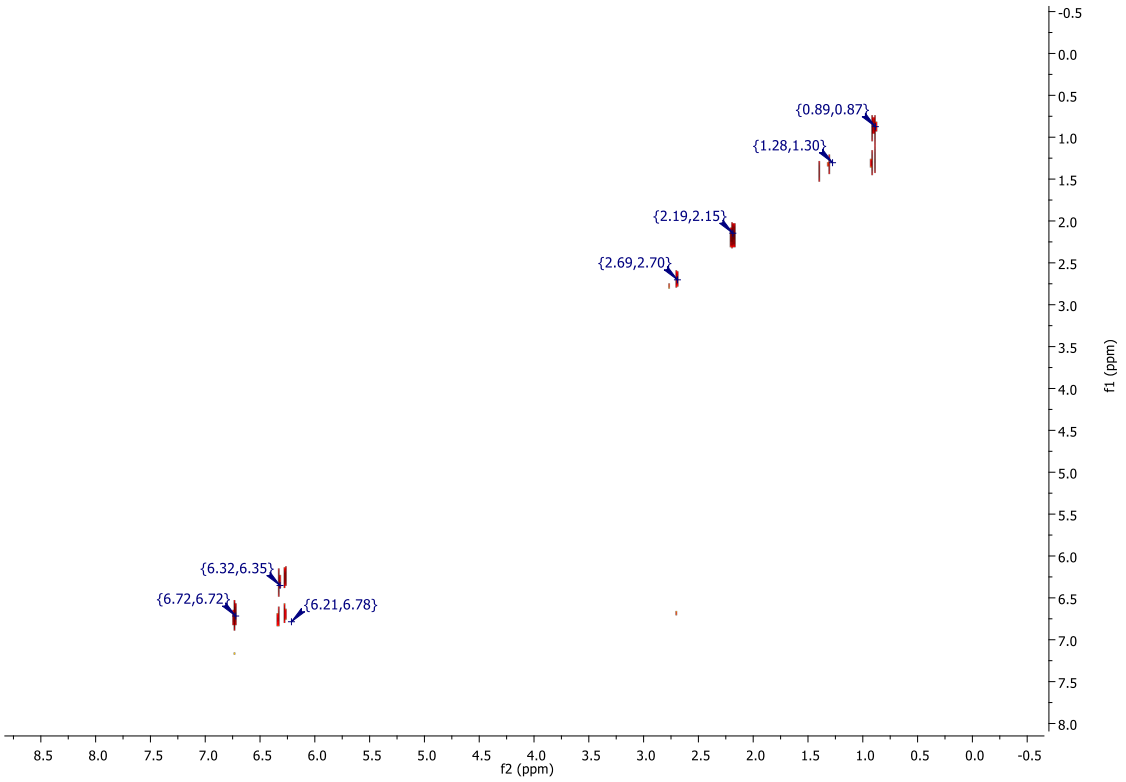

Figure S16: ^{1}H-^{1}H COSY (500 MHz) of **1** in $CDCl_3$, showing that none of the signals observed by ^{1}H NMR are coupled to one another. Correlation seen at 0.89 ppm is residual pentane solvent.

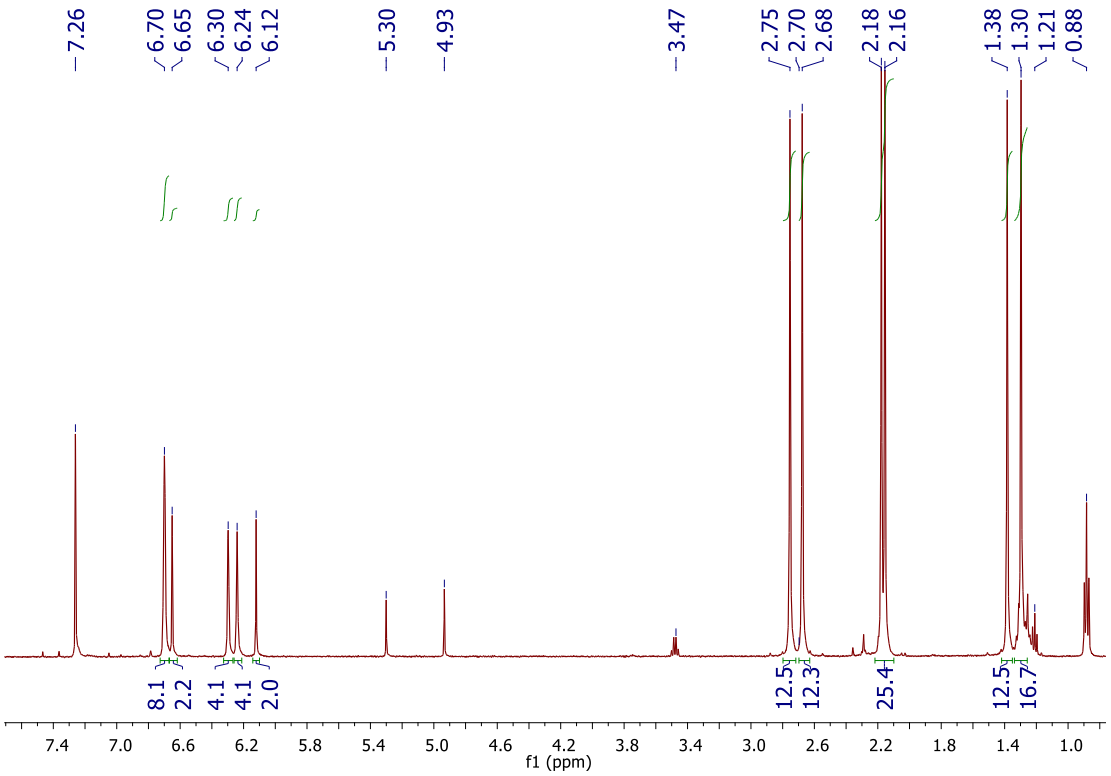

Figure S17: ^{1}H NMR (500 MHz) of **1** in $CDCl_3$ sample used for ^{1}H-^{1}H COSY experiment in Figure S16. Peaks observed at the following chemical shifts are residual solvents in sample: 0.88 ppm (pentane), 1.21 ppm and 3.47 ppm (diethyl ether), 4.93 ppm (dibromomethane), 5.30 ppm (dichloromethane).

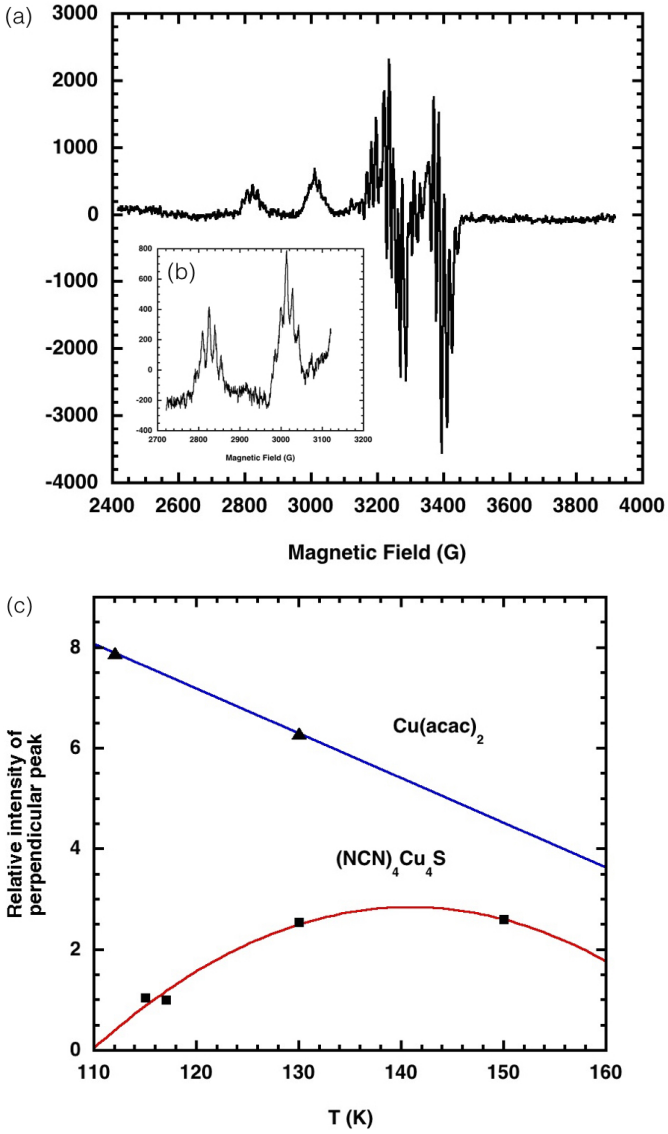

Figure S18. (a) X-band EPR spectrum of **1** in toluene glass at 115 K; (b) the $g_{\|}$ region of the EPR spectrum; (c) temperature dependence of EPR signal intensity for **1** and for a $Cu(acac)_2$ control, with curves drawn to guide the eye.